ORNL/TM-2018/1048

Double-Sided Pressureless-Sintered-Silver Interconnects Fabricated by Reflow-Oven-Processing

Andrew A. Wereszczak
Branndon R. Chen
Osama M. Jadaan
Brian A. Oistad

October 2018

Approved for public release.
Distribution is unlimited.

OAK RIDGE NATIONAL LABORATORY
MANAGED BY UT-BATTELLE FOR THE US DEPARTMENT OF ENERGY

ORNL/TM-2018/1048

Materials Science and Technology Division

Double-Sided Pressureless-Sintered-Silver-Interconnects Fabricated by Reflow-Oven-Processing

Andrew A. Wereszczak
Branndon R. Chen
Osama M. Jadaan
Brian A. Oistad

October 2018

Prepared by
OAK RIDGE NATIONAL LABORATORY
Oak Ridge, TN 37831-6283
managed by
UT-BATTELLE, LLC
for the
US DEPARTMENT OF ENERGY
under contract DE-AC05-00OR22725

CONTENTS

LIST OF FIGURES

LIST OF TABLES

ACKNOWLEDGMENTS

Research sponsored by the Electric Drive Technologies Programs, DOE Vehicle Technologies Office, under contract DE-AC05-00OR22725 with UT-Battelle, LLC. The authors thank USDOE's S. Rogers and ORNL's B. Ozpineci for their financial and programmatic support, S. Campbell for assistance with the reflow oven, R. Wiles for CAD assistance, and S. Chowdhury, E. Gurpinar, and E. Lara-Curzio for their reviews and helpful input.

ABSTRACT

A significant amount of development with sintered-silver as an alternative interconnect (or attachment or attach) material in power electronic devices has occurred since ~ 2010 at Oak Ridge National Laboratory's National Transportation Research Center. Continuous sponsorship of the work enabled improvements and understanding of several sequential processing steps which otherwise would not have occurred with a short duration or an intermittently funded project. The majority of that work has occurred with a focus on improving its processing and consequential mechanical reliability of the interconnect while promoting adaptability to power electronic device manufacturing. The work includes determining application issues of silver-sintering and the developing processes that would make it amenable for use with reflow oven sintering. As part of that work, co-development of maximum interconnect strength of the sintered-silver interconnect occurred, and that also involved examining candidate plating materials that could be used in concert with them for the "interconnect system". All of this work involved the consideration of a single sintered-silver interconnect.

For the next step in the development sequence, interest turned to adapting previous experiences to the processing of "double-sided silver-sintering" involving the concurrent sintering of two separate interconnects in a system, which is the main focus of this report. An example of this would be bonding two interconnects to a dual-sided die. The processing of two interconnects is nearly identical to the processing of a single interconnect; however, the shear-testing mechanical evaluation is more complex, so consideration was needed for testing two interconnects at different times.

This report describes the process of mechanical testing and evaluation of concurrent sintering of two silver interconnects along with the usage of heating method (reflow oven) process to demonstrate good quality interconnects and easy manufacturing process.

1. INTRODUCTION

There are several attractive characteristics that result in sintered-silver (Ag) to be a strong candidate material for interconnects in power electronic devices. Sintered-Ag has high electrical and thermal conductivities, has high-temperature capability, and the material is Restriction of Hazardous Substances (RoHS) compliant. The reader is directed toward Siow's review [1] which provides an informative and thorough review of sintered-silver technology.

Despite its recognized attributes, the more widespread acceptance of sintered-Ag for interconnects has been somewhat slow; sintered-Ag's different characteristics and manner of processing are primary reasons for that. Its solid-state processing and the potential need for pressure assistance represent challenges to solder interconnect practitioners. Additionally, conversion to Ag-sintering technology is hindered when Ag-paste manufacturers tend to only provide recommended guidelines for sintering profiles for specific (small) size bond area or leave the responsibility of identifying sintering profiles to the user based on the user's experience, application requirements, and sintering equipment. The use of reflow oven technology is common for processing solder-based interconnects*, and being that solders have been the workhorse for such bonding for decades, interconnect processing practitioners are therefore familiar with that method of heating.

* The word "interconnect" is used in this report, but it may be interpreted to be synonymous with "attachment" or "attach" which may by preferred by others in the electronic packaging community.

To help address this, attention has been devoted at Oak Ridge National Laboratory (ORNL)'s National Transportation Research Center (NTRC). Research has been conducted for nearly 10 years to advance the fabrication of Ag-sintering interconnects including using a reflow oven. The use of a reflow oven essentially mandates the pressureless sintering process of Ag interconnect; this paradigm was counter to the advocation of pressure-assistance with Ag-sintering that existed. The early work studied many practical yet general aspects of processing Ag-sintered interconnects [2-4]. When attention was directed toward the prospect of using reflow oven technology for pressureless sintering of silver interconnects, it was recognized by the authors that pre-drying printed silver pastes prior to their insertion into a reflow oven was needed because the paste manufacturers had not evidently examined such a step. A drying method was developed at ORNL's NTRC based on contact heating, and a schematic of such is shown in Fig. 1 [5]. Pre-sinter-drying removes the majority of the paste's solvent but maintains a level of tackiness that promotes bonding with the surface of the to-be-mated object (e.g., a die). This pre-drying step has significantly improved the strength of interconnects (shear strengths > 40 MPa) for sintering using reflow oven processing [6]. Attention was also given to the choice and compatibilities of plating materials with Ag-sintered interconnects [7], and the interpretation of failure stress of Ag-sintered interconnects depending on the geometry of the mating structures it is bonded to [8].

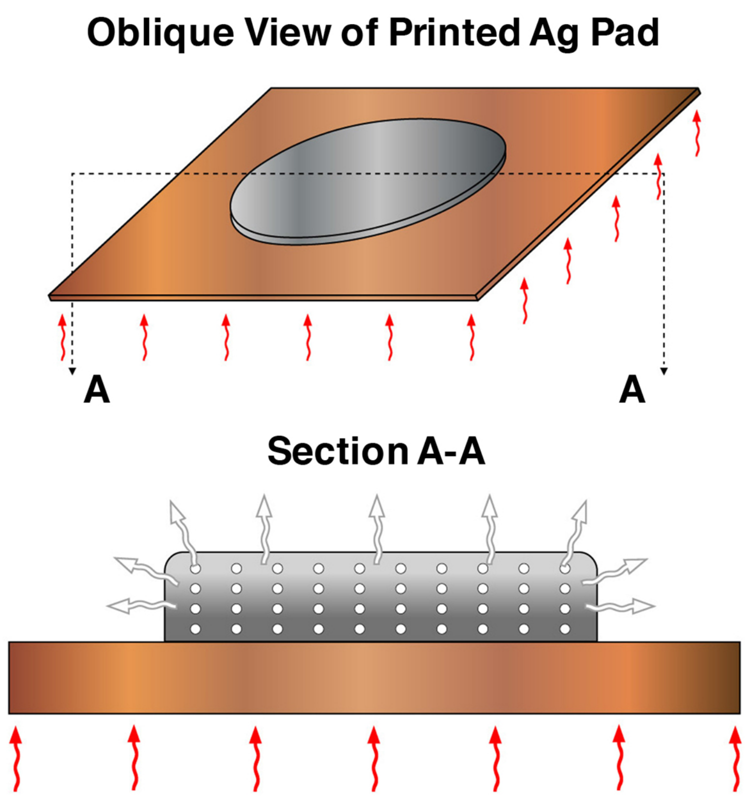

Figure 1. Schematic of the contact-drying of the printed silver. Red and white arrows represent direction and location of heating, and the direction and location of the solvent evaporation, respectively.

The present study and report are associated with a contemporary and additional technology, and the prospect of Ag-sintering both sides of a power semiconductor die in a power module. Double-sided module enables extraction of heat generated by the power semiconductors from both sides of the module for increased thermal performance. The potential processing of double sided sintered die is nearly identical to the processing of a single sided sintered die; however, the shear-testing mechanical evaluation is more complex, so consideration was needed for testing two interconnects at different times. *This study describes the concurrent sintering of two silver interconnects, the description of their mechanical testing and evaluation, and ultimately the demonstration of the processing of two good quality interconnects using a heating method (reflow oven) that makes this a quite manufacturable process.*

2. EXPERIMENTAL APPROACH

2.1 Sintered-Ag Interconnect Processing

Pre-sintering Processes

This subsection describes the pre-Ag-sintering processes that were used to prepare samples for 250°C-sintering in the reflow oven - samples that had two interconnects in them. All sintering occurred immediately after the contact-drying was completed, and both contact-drying and sintering were done in the same laboratory and were subjected to the same ambient air conditions (22°C and 55% relative humidity). The process included the printing of the wet Ag paste, its open-face contact-drying, and assembly of DBC substrate sandwiches where the printed and dried (to-be-sintered) Ag pad interconnect comprises the center of the DBC substrate sandwich.

The printing and drying methods used are described in Ref. [5] and are summarized as follows.

- *Printing*: Printing was done using a commercially available Ag paste (Loctite Ablestik SSP 2020 [9-10][†], Batch# 026K995195, Henkel Electronic Materials LLC, Irvine, CA) and a stencil having a 0.102 mm thickness and a 5-mm-diameter circular print (UTZ Technologies, Little Falls, NJ). The circular print was centered on a face of the 12.7 mm × 12.7 mm direct bonded copper (DBC) ceramic substrate surface. The DBC ceramic substrate had a 0.3mm-thick copper cladding and a 0.6mm-thick aluminum oxide ceramic. The copper cladding was plated with electroless nickel immersion gold (ENIG) by the substrate vendor (Remtec, Norwood, MA). The ENIG plating had a manufacturer-reported mid-phosphorus (P), nickel (6–10% P) pre-plate layer thickness of approximately 3–7 μm and a gold (Au) finish plating of about 0.05 μm.

- *Drying*: Contact-drying of the wet, printed Ag paste was done with a hot plate set at 65°C for 130 seconds in ambient air. That combination of drying temperature and time was identified as providing a suitable compromise of (1) sufficient removal of the paste's solvent, (2) tackiness for wet-adherence to the substrate, and (3) stiffness, so that the Ag print shape exhibited less than 5% dimensional changes during its upcoming, room-temperature compressive setting. A hot plate (Quick870, Madell Technology Corporation, Ontario, CA) was used to produce the contact heating

[†] Certain commercial materials or equipment are identified in this paper to adequately describe the experimental procedure. This does not imply their endorsement by the Oak Ridge National Laboratory, UT-Battelle, the US Department of Energy, nor Oak Ridge Associated Universities nor that these materials and equipment are necessarily the best choices for these purposes.

for this drying method, and its surface temperature was measured using an external K-type thermocouple.‡

Consolidation occurred after the pastes were contact-dried, and it is schematically shown in Figs. 2-3. A DBC substrate sandwich specimen comprised of three DBC substrates and the contact-dried Ag-print between the DBC substrates. The specimen was then formed with the aid of an alignment fixture that promoted concentricity during both dried-paste setting and follow-on sintering. These DBC substrate sandwiches were used in this study because they can mechanically withstand the application of the high-contact-loads necessary to cause shear failure of the 5-mm-diameter sintered-Ag interconnect. A 11-kPa compressive stress was then applied for 3 seconds onto the consolidated DBC substrate sandwich to set the contact-dried Ag print against both DBC substrates; this is analogous to the setting force associated with a pick-and-place operation.§

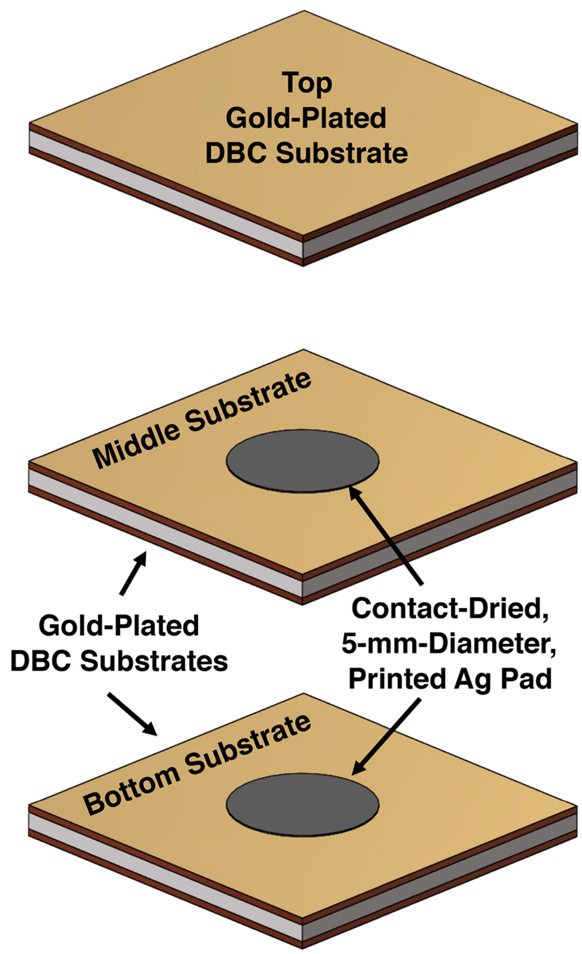

Figure 2. Exploded view of the double-sided DBC substrate sandwich prior to assembly.

‡ Optimal drying times and temperatures are dependent on the combination of user chosen Ag paste, print size, underlayment, and heating apparatus. Therefore, it should not be assumed that the present study's identified optimized drying time and temperature will also be the same for any deviation from the Ag paste, print size, underlayment, and heating apparatus described here.

§ 11 KPa equates to an available dead weight (0.22 N) that was used to compress the interconnect area (20 mm^2), and was determined from the Ag-paste's contact drying examination.

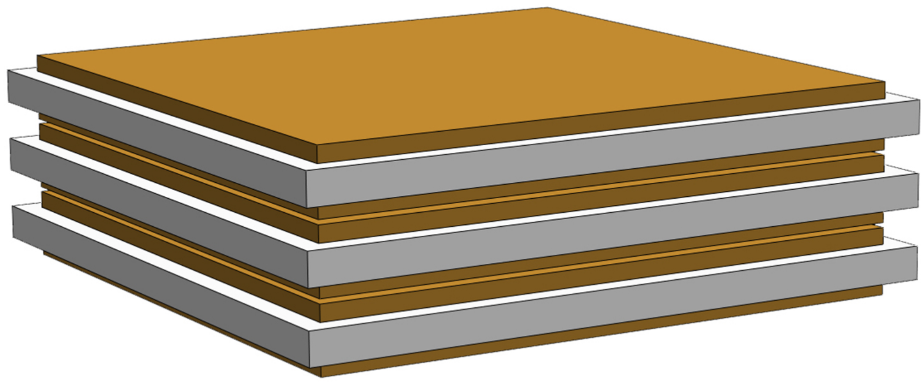

Figure 3. Schematic of the assembled double-sided DBC substrate sandwich.

Reflow-Oven- and Static-Convection-Oven-Sintering

A four-zone, convection-type reflow oven (Sikama FALCON 5/C, Sikama International Inc., Santa Barbara, CA) was used to sinter the contact-dried DBC substrate sandwiches. Sintering was done in ambient air (22°C and 55% relatively humidity). The reflow oven and the alignment of the DBC substrate sandwiches entering the oven are shown in Figs. 4-5, respectively. The target (and programmed) temperatures of the four oven zones were 75°C (75°C), 100°C (75°C), 250°C (262°C), and 250°C (260°C). Independent thermocouple measurements were used to identify what those set point temperatures needed to be. The oven's conveyer speed was set to 20 cm/min in between zones and dwelled in each for 30 min. The fabricated samples are shown in Fig. 6.

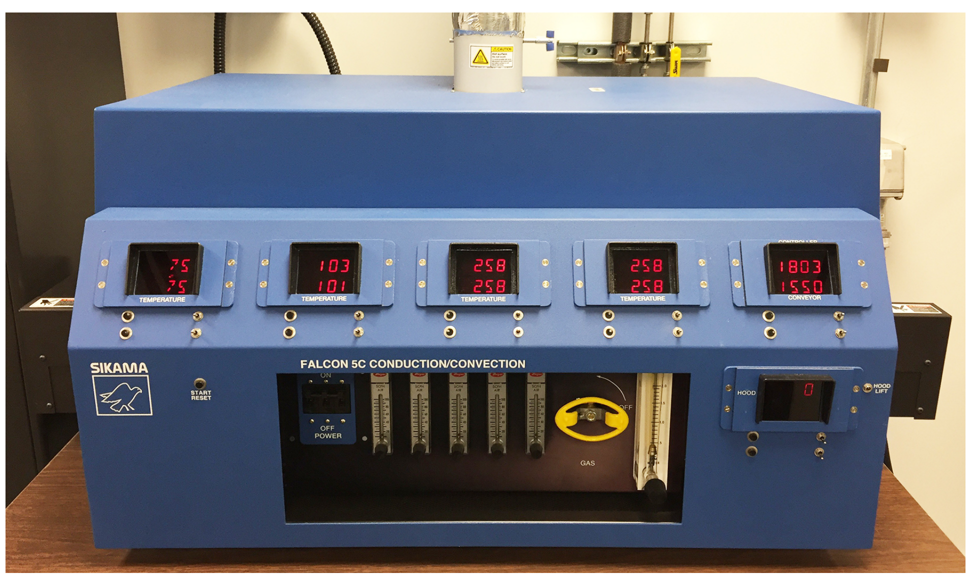

Figure 4. Reflow oven used for the double-sided pressureless sintering of the silver interconnect.

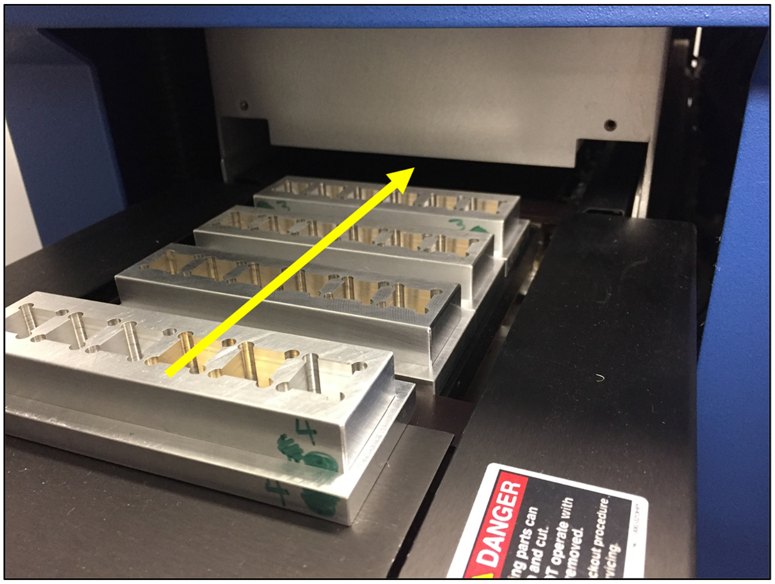

Figure 5. Fixtures were used to carry and transfer DBC substrate sandwiches through the reflow oven during sintering as well as concentrically align them during their setting process.

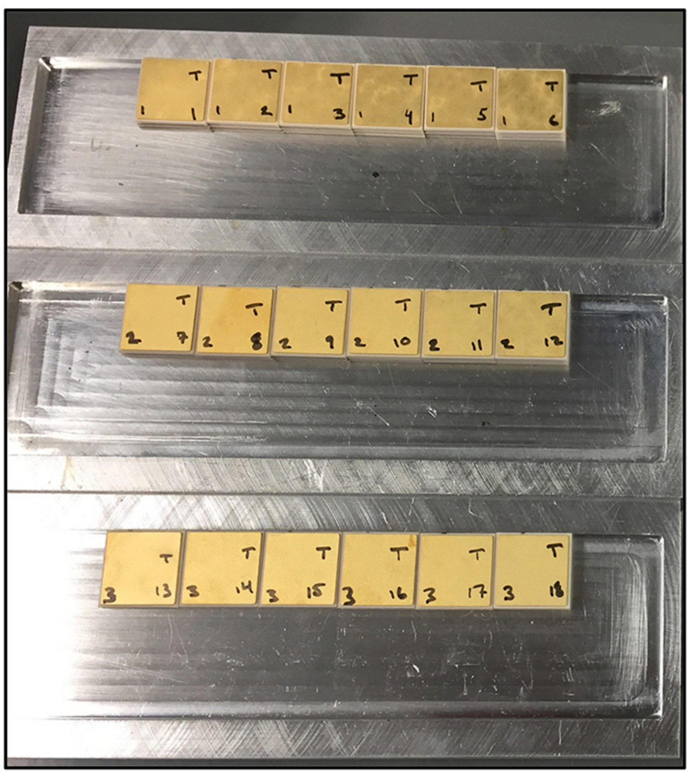

Figure 6. Fabricated specimens. Each shown square is 12.7 x 12.7 mm.

2.2 Mechanical Testing and Analysis

Mechanical testing of the DBC substrate sandwiches were performed in two steps using a commercial shear tester (4000 Bondtester, Nordson Dage, Fremont, CA). All testing was done at room temperature.

The "Test 1" configuration is schematically shown in Fig. 7 and occurred when all three of the substrates were still bonded to one another. The bottom substrate was gripped at two of its ends using a vice fixture while a shear testing tool horizontally contacted the top substrate. Horizontal loading occurred at a displacement rate of 25 µm/s applying a continually increasing uniaxially induced shear stress to each specimen's interconnect until failure resulted. The bottom of the shear testing tool was positioned at a height that was aligned with the bottom of the aluminum oxide substrate of the top DBC substrate. The force at failure was recorded for each test (two tests per specimen).

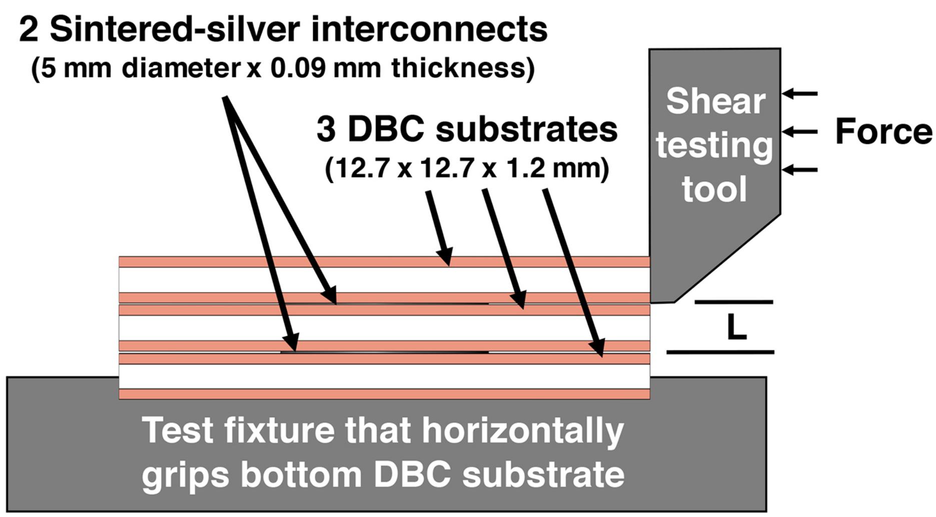

Figure 7. Side-view schematic of the Test 1 configuration. It consisted of three substrates and two sintered-Ag interconnects, and failure would occur within the bottom interconnect. The moment arm, L, to the middle of the bottom interconnect is the sum (1.335 mm) of the thicknesses of the top interconnect (0.09 mm), the middle DBC substrate (1.20 mm), and the half-height (0.045 mm) of the bottom interconnect. (Interconnect dimensions were verified with micrometer.)

Referring to Fig. 7 and the described Test 1 configuration, failure always occurred at the interconnect that bonded the (gripped) bottom substrate and the middle substrate. Failure initiation occurs there because of a relatively high tensile stress (and not shear) for reasons associated with the test configuration (i.e., a relatively large moment arm, L) and that were explained in Ref. [8].

Each specimen's tensile stress at failure, *S,* for the Test 1 configuration was then calculated according to:

$$S = \frac{4\, L\, P_{max}}{\pi\, r^3} \quad , \qquad (1)$$

where L is the moment arm length (= 1.335 mm) as indicated in Fig. 7, P_{max} is the measured failure force, and r is the radius of the interconnect's circular pad (= 2.5 mm).

The "Test 2" configuration is schematically shown in Fig. 8 and was used to test the interconnect of the surviving pair of substrates after the Test 1 configuration had been completed. The force at failure was recorded for each test.

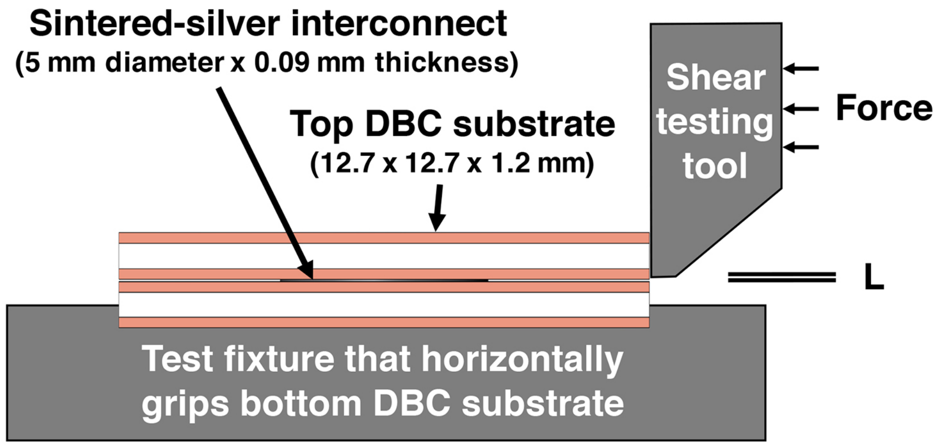

Figure 8. Schematic of the Test 2 configuration. It constitutes the testing of the pair of bonded DBC substrates that survived Test 1 loading and consisted of two substrates and one sintered-Ag interconnect. The moment arm, L, is the half-height (0.045 mm) of the interconnect and is only about 3% that of the Test 1 configuration moment arm.

For the Test 2 configuration, each specimen's maximum shear stress at failure, τ_{max}, was calculated using the combination of the moment of inertia of a circle (i.e., the printed sintered-Ag pad shape) and the expression for maximum shear stress [11] shown in Eq. 2:

$$\tau_{max} = \frac{P_{max}(3+2\nu)}{2\pi(1+\nu)r^2}, \tag{2}$$

where P_{max} is the recorded failure force, ν is the Poisson's ratio of the sintered-Ag (taken as = 0.15 here for 50% porosity [3]), and r is the circular print-pad's radius (= 2.5 mm) of the interconnect. The maximum stress calculated using Eq. 2 is 7.6% larger than the average stress calculated using the classical beam equation for shear and a circular shape (i.e., $\tau_{max} = 4P_{max}/3\pi r^2$), so Eq. 2 is preferentially used because the Poisson's effect is not considered in the classical beam equation and because failure initiation will almost always occur from a maximum applied stress and not an average stress [8].

The reason tensile failure stress was calculated for the Test 1 configuration and shear failure stress was instead calculated for the Test 2 configuration has the following explanation. When Eqs. 1-2 are equated and the L/r ratio is determined as a function of Poisson's ratio or

$$\frac{L}{r} = \frac{(3+2\nu)}{8\,(1+\nu)}, \tag{3}$$

then two regions can be identified as illustrated in Fig. 9 where tensile stress is greater than shear stress or vice versa.

A two-parameter Weibull distribution and also a Gaussian distribution were fitted to the tensile failure stresses (Eq. 1) and the shear failure stresses (Eq. 2) using commercially available software (WeibPar, Connecticut Reserve Technologies, Gates Mills, OH).

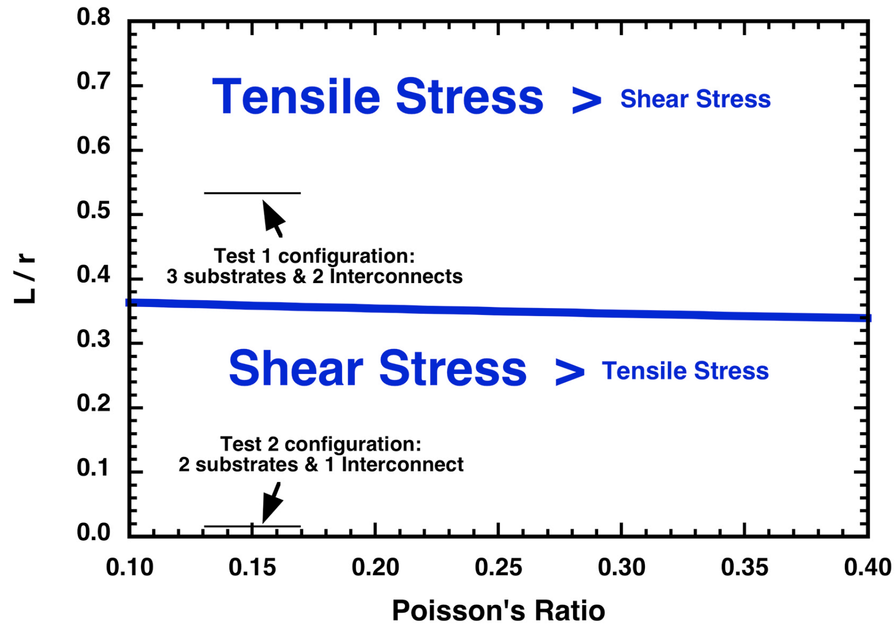

Figure 9. L/r as a function of Poisson's ratio according to Eq. 3. Tensile stress is greater than shear stress for L/r values greater than this function, and vice-versa for L/r values below less than it. The L/r values for the Test 1 and Test 2 configurations show that tension dominated for the former and shear for the latter.

3. RESULTS AND DISCUSSIONS

The tensile failure stress and shear failure stress distributions from Tests 1 and 2 are shown in Figs. 10 and 11, respectively, and their summarized Weibull and Gaussian parameters are listed in Table 1. The characteristic tensile failure stress for Test 1 was approximately 47 MPa and the characteristic failure shear stress for Test 2 was approximately 41 MPa. The characteristic shear failure stress value is equivalent to that of similar examinations conducted by ORNL [5-7]. Their Weibull moduli were equivalent indicating the amount of scatter of their distributions were also equivalent.

There was an equal shear stress applied to both interconnects in the Test 1 configuration during each specimen's mechanical testing. Using Eq. 2 to calculate that shear stress for a given failure force and comparing that to the calculated tensile failure stress using Eq. 1, one determines that the shear stress at failure is 50% (for a Poisson's ratio = 0.15) of the tensile stress at failure. Therefore, the characteristic tensile stress at failure for the Test 1 configuration of ~ 47 MPa means there was a shear stress at failure of approximately 24 MPa. The characteristic shear failure force for the Test 2 configuration was ~ 41 MPa, and it should be higher valued than what was imposed during the Test 1 configuration, otherwise, one of the two interconnects would have failed from shear instead.

Failure analysis has been performed on the same sintered-silver-gold-plated interconnects [7] examined in the present study, and shear failures were adhesive because they failed at the interface between the sintered-silver and the plating. Adhesive failures were expected in the test specimens in this study.

The achievement of high failure stresses for both interconnects demonstrates that reflow-oven-processing can be used to effectively to fabricate pressureless sintered-silver interconnects. If they were to be used in double-sided cooled power modules, then the high thermal conductivity of sintered-silver could enable excellent thermal management of the device.

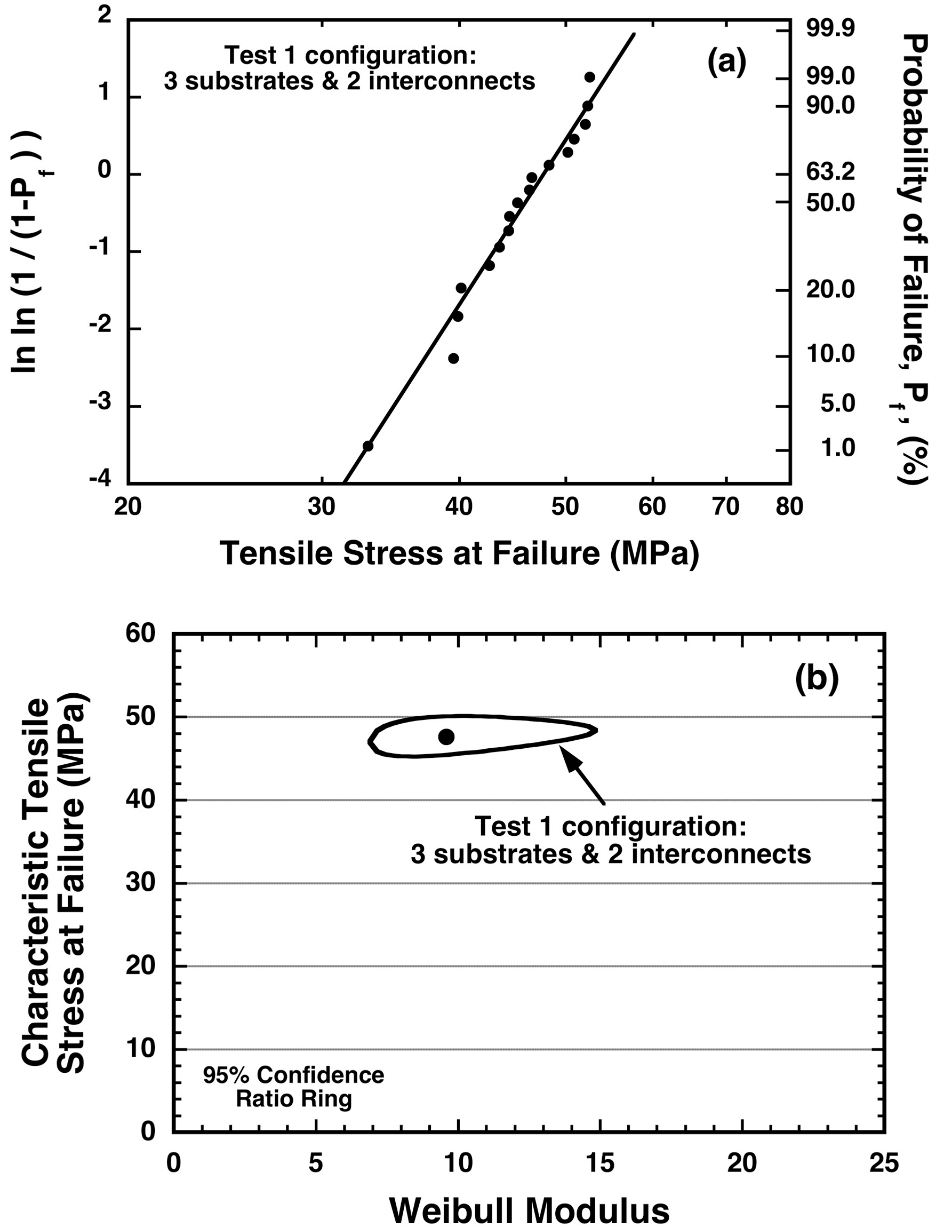

Test 1 configuration:
3 substrates & 2 interconnects
(a)
ln ln (1 / (1-P_f))
Probability of Failure, P_f , (%)
Tensile Stress at Failure (MPa)
2
1
0
-1
-2
-3
-4
99.9
99.0
90.0
63.2
50.0
20.0
10.0
5.0
1.0
20
30
40
50
60
70
80
(b)
Characteristic Tensile
Stress at Failure (MPa)
Test 1 configuration:
3 substrates & 2 interconnects
95% Confidence
Ratio Ring
Weibull Modulus
60
50
40
30
20
10
0
5
10
15
20
25

Figure 10. Weibull distribution (a) tensile failure stress data and (b) 95% confidence ratio ring for the Test 1 configuration tested at 25°C.

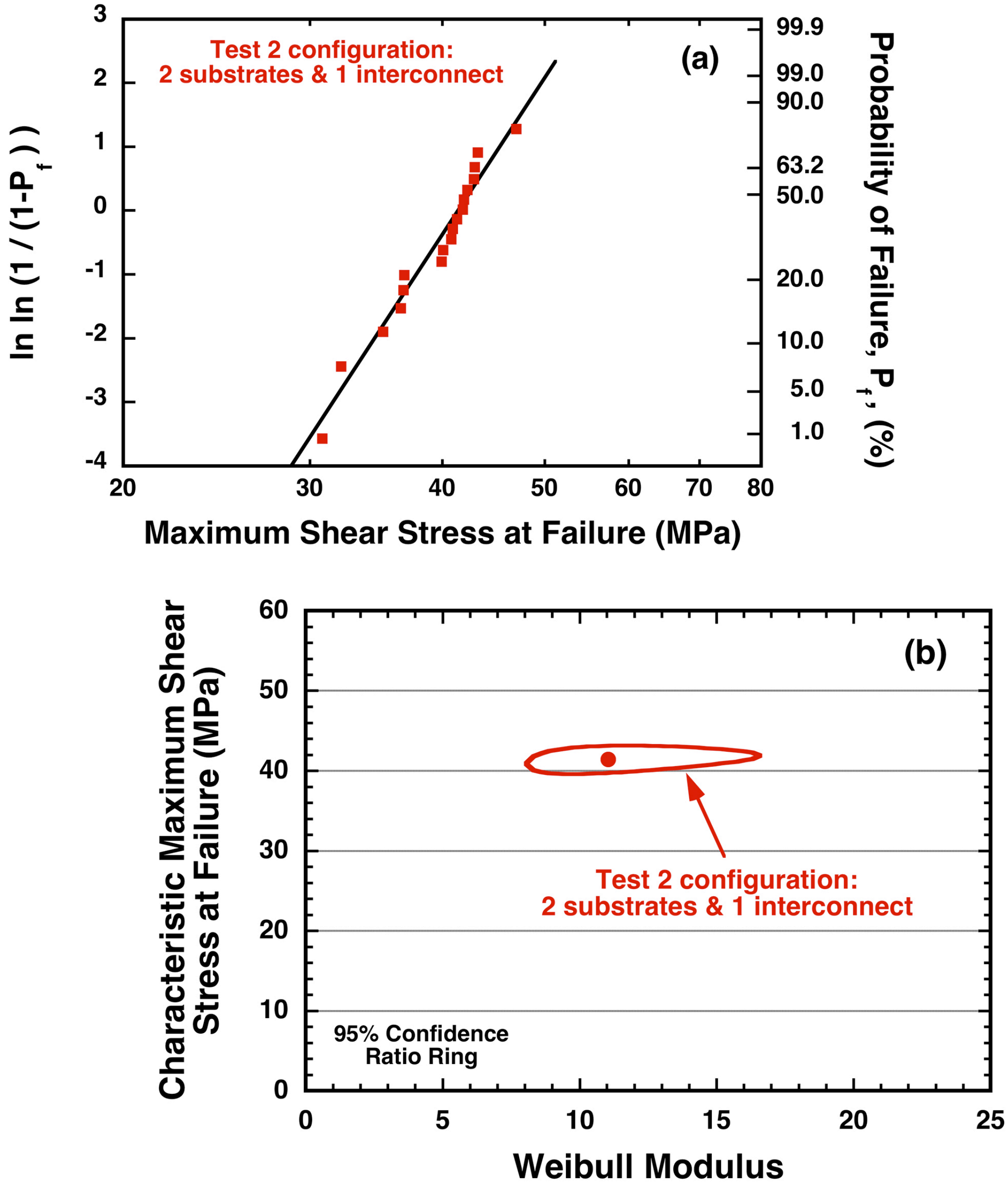

Figure 11. Weibull distribution (a) shear failure stress data and (b) 95% confidence ratio ring for the Test 2 configuration tested at 25°C.

Table 1. Values of two-parameter Weibull and Gaussian distributions for the measured maximum shear failure stress for the silver interconnects sintered in the two different ovens. Values in square brackets for the Weibull parameters represent 95% confidence bounds.

Testing Configuration	Weibull		Gaussian	
	Characteristic Maximum Failure Stress (MPa)	Modulus	Average Maximum Failure Stress (MPa)	Standard Deviation
Test 1 (Tensile)	46.6 [44.9, 50.1]	10.1 [6.3, 13.5]	45.4	5.4
Test 2 (Shear)	41.4 [39.5, 43.3]	11.9 [7.5, 16.1]	39.6	4.1

4. CONCLUSIONS

Pre-sinter-drying of printed silver paste has enabled pressureless silver sintering to achieve shear strengths greater than 40 MPa using reflow oven heating. Those high strengths are a consequence of careful processing that includes contact-drying followed by reflow oven processing methods developed at ORNL during the last few years. This process can be adopted for double sided interconnects to achieve better thermal capabilities.

5. REFERENCES

[1] K. S. Siow, "Are Sintered Silver Joints Ready for Use as Interconnect Material in Microelectronic Packaging?", *Journal of Electronic Materials*, 43:947-961, (2014), doi: 10.1007/s11664-013-2967-3.

[2] A. A. Wereszczak, D. J. Vuono, Z. Liang, and E. E. Fox, "Sintered Silver Joint Strength Dependence on Substrate Topography and Attachment Pad Geometry," 7th International Conference on Integrated Power Electronics Systems (CIPS), Nuremberg, Germany, Mar. 2012, ISBN: 978-3-8007-3414-6.

[3] A. A. Wereszczak, Z. Liang, M. K. Ferber, and L. D. Marlino, "Uniqueness and Challenges of Sintered Silver as a Bonded Interface Material," *Journal of Microelectronics and Electronic Packaging*, 11:158-165, (2014), doi: 10.4071/imaps.429.

[4] A. A. Wereszczak, M. C. Modugno, S. B. Waters, D. J. DeVoto, and P. P. Paret, "Method to Determine Maximum Allowable Sinterable Silver Interconnect Size," pp. 207-215 in *IMAPS HiTEC 2016*, Paper WP23, Albuquerque, NM, 2016, doi: 10.4071/2016-HITEC-207.

[5] A. A. Wereszczak, M. C. Modugno, B. R. Chen, and W. M. Carty, "Contact Drying of Printed Sinterable-Silver Paste," *IEEE Transactions on Components, Packaging and Manufacturing Technology*, 7:2079-2086, (2017), doi:10.1109/TCPMT.2017.2752140.

[6] Wereszczak, A. A., Chen, B. R., and Oistad, B. A., "Reflow-Oven-Processing of Pressureless Sintered-Silver Interconnects," *Journal of Materials Processing Technology*, 255:500-506, (2018), doi:10.1016/j.jmatprotec.2018.01.001.

[7] A. A. Wereszczak, B. R. Chen, B. A. Oistad, S. B. Waters, and A. T. Mayville, "Failure Stress Comparison of Different Pairings of Ag-Plating and Reflow-Oven-Processed Pressurelessly-Sintered-Ag Interconnects," in press, *Journal of Materials Science: Materials in Electronics*, (2018), doi: 10.1007/s10854-018-0151-5.

[8] A. A. Wereszczak, B. R. Chen, O. M. Jadaan, B. A. Oistad, M. C. Modugno, J. W. Sharp, and J. R. and Salvador, "Cantilever Testing of Sintered-Silver Interconnects," *Journal of Materials Science: Materials in Electronics*, 29:1530-1541 (2018), doi: 10.1007/s10854-017-8063-3.
[9] LOCTITE ABLESTIK SSP 2020, Henkel Corporation, Safety Data Sheet, October 2014.
[10] LOCTITE ABLESTIK SSP 2020, Henkel Corporation, Technical Data Sheet, December 2012.
[11] J. N. Goodier and S. P. Timoshenko, *Theory of Elasticity*, 3rd Edition, Mc-Graw-Hill Education, New York, 1970.